J. Fluid Mech. (1979), *vol.* 90, *part* 2, *pp.* 377–395
Printed in Great Britain

Bénard convection in a finite box: secondary and imperfect bifurcations

By P. HALL AND I. C. WALTON
Department of Mathematics, Imperial College, London

(Received 20 January 1978)

In the solution given by Hall & Walton (1977) for Bénard convection in a two-dimensional box with slightly imperfectly insulated side walls it was shown that there were certain critical values $2L_c$ of the length $2L$ of the box at which two modes became unstable simultaneously. In this paper we show that in the neighbourhood of L_c a secondary transition takes place which may be a bifurcation or a smooth transition depending on the boundary conditions.

1. Introduction

The onset of convection in a two-dimensional rectangular box has recently been the focus of much attention. Drazin (1975) discussed the flow in a box whose horizontal surfaces were stress-free and isothermal and whose vertical boundaries were rigid and perfectly insulated. He showed that the critical value of the Rayleigh number at which instability sets in is $R_c = R_c(L)$ with $R_c(L) > R_c^\infty$, the corresponding value when the box is unbounded in the horizontal directions. This theory was extended by Hall & Walton (1977, hereafter referred to as HW) and Daniels (1977) to include imperfectly insulated vertical boundaries.

HW showed that for the perfect problem two modes (one even, one odd) become unstable almost simultaneously. In fact for large values of L, the half-length of the box, their critical Rayleigh numbers differ only by a term $O(L^{-3})$ and furthermore become equal at certain discrete finite values of L. The theory given by HW is strictly valid only in the neighbourhood of the first bifurcation and for some values of L this is very small indeed. In this paper we extend that work to cover a larger range of values of R including both bifurcations but still subject to the constraint $R - R_c(L) \ll L^{-2}$ imposed in HW.

The problem is formulated in § 2 and in § 3 we give a summary of Drazin's linear stability analysis of the perfect problem. The linear and nonlinear stability of the imperfect problem is discussed in § 4, and the amplitudes A and B of the even and odd modes are shown to satisfy equations of the form

$$\left.\begin{aligned} c_5\,dA/dt &= c_1(A^3 + c_2 A^2 B - c_3(R_1 - \mu) + c_4), \\ d_5\,dB/dt &= d_1(B^3 + d_2 B^2 A - d_3 R_1 + d_4). \end{aligned}\right\} \tag{1.1}$$

Here c_i, d_i ($i = 1, \ldots, 5$) and μ are constants depending on L, and R_1 is a scaled Rayleigh number. When the side walls are perfect insulators $c_4 = d_4 = 0$ and (1.1) then reduces to a pair of equations examined by Keener (1976). In § 5 we discuss the solutions of these equations in the context of Bénard convection and in § 6 we allow c_4 and d_4 to be non-zero. Finally, the results are discussed in § 7.

2. Formulation of the problem

We consider two-dimensional convection in a rectangular box bounded vertically and in one horizontal direction; the box is assumed to be of infinite extent in the second horizontal direction. The vertical side walls are taken to be rigid and almost perfect insulators. The upper and lower surfaces are taken to be free and isothermal, the lower surface being maintained at a temperature ΔT above that of the upper one.

Let (x, z) be dimensionless horizontal and vertical co-ordinates so chosen that the upper and lower surfaces are located at $z = 0, 1$ and the vertical boundaries at $x = \pm L$. If T is a dimensionless temperature and Ψ a dimensionless stream function, the equations governing the motion are (Kelly & Pal 1976)

$$\nabla^2(\nabla^2 - \partial/\partial t)\Psi = R\,\partial T/\partial x + \sigma^{-1}\partial(\nabla^2\Psi, \Psi)/\partial(x, z), \tag{2.1}$$

$$(\nabla^2 - \sigma\,\partial/\partial t)\,T = \partial(T, \Psi)/\partial(x, z), \tag{2.2}$$

where the Rayleigh number R and Prandtl number σ are defined by

$$R = g\alpha(\Delta T)\,h^3/\nu\kappa, \quad \sigma = \nu/\kappa. \tag{2.3a,b}$$

Here ν, κ and α are the coefficients of kinematic viscosity, thermal diffusivity and thermal expansion, respectively, and h is the separation of the horizontal surfaces. In deriving (2.1) and (2.2), it is assumed that the fluid is incompressible and the Boussinesq approximation has been made.

The boundary conditions needed to complete the specification of the problem are

$$\left.\begin{aligned} \Psi = \partial^2\Psi/\partial z^2 = 0, \quad T = 1, 0 \quad \text{at} \quad z = 0, 1; \\ \Psi = \partial\Psi/\partial x = 0 \quad \text{at} \quad x = \pm L; \\ \partial T/\partial x = \beta g(z) \quad \text{at} \quad x = L; \\ \partial T/\partial x = \beta h(z) \quad \text{at} \quad x = -L. \end{aligned}\right\} \tag{2.4}$$

Thus β is the characteristic scale of the deviation of the boundary conditions from those for perfectly insulated side walls; the functions $g(z)$ and $h(z)$ are prescribed.

3. Linear stability with perfectly insulated boundaries

The stability of the flow with $\beta = 0$ has been discussed within the restrictions of linear theory by Drazin (1975). In view of our extensive use of his solution later on, it is worthwhile repeating the salient features of his work here.

We first note that a simple steady solution of (2.1), (2.2) and (2.4) is

$$T = 1 - z, \quad \Psi \equiv 0.$$

We perturb this state by writing

$$T = 1 - z + \theta, \quad \Psi = \psi,$$

where θ and ψ are small; then the linearized equations which determine these functions are

$$\nabla^2(\nabla^2 - \partial/\partial t)\,\psi = R\,\partial\theta/\partial x, \quad (\nabla^2 - \sigma\,\partial/\partial t)\,\theta = \partial\psi/\partial x, \tag{3.1}$$

with boundary conditions

$$\left.\begin{aligned} \theta = \psi = \partial^2\psi/\partial z^2 = 0 \quad \text{at} \quad z = 0, 1, \\ \partial\theta/\partial x = \psi = \partial\psi/\partial x = 0 \quad \text{at} \quad x = \pm L. \end{aligned}\right\} \tag{3.2}$$

Here $\nabla^2 \equiv \partial^2/\partial x^2 + \partial^2/\partial z^2$. The boundary conditions (3.2) suggest that we may seek a neutrally stable solution of (3.1) of the form

$$(\theta, \psi) = (\theta_D(x), \psi_D(x)) \sin n\pi z, \tag{3.3}$$

where θ_D and ψ_D are given by

$$\left.\begin{aligned}(d^2/dx^2 - n^2\pi^2)^2 \psi_D &= R\, d\theta_D/dx,\\ (d^2/dx^2 - n^2\pi^2)\,\theta_D &= d\psi_D/dx,\end{aligned}\right\} \tag{3.4}$$

with

$$d\theta_D/dx = \psi_D = d\psi_D/dx = 0 \quad \text{at} \quad x = \pm L. \tag{3.5}$$

The general solution to (3.4) is

$$\theta_D = \sum_{i=1}^{3} (A_{in} \cos a_{in} x + B_{in} \sin a_{in} x), \quad \psi_D = \sum_{i=1}^{3} (C_{in} \cos a_{in} x + D_{in} \sin a_{in} x), \tag{3.6}$$

where A_{in}, B_{in}, C_{in} and D_{in} are constants and the wavenumbers a_{in} are the three roots of

$$(a^2 + n^2\pi^2)^3 = Ra^2 \tag{3.7}$$

which have arguments in the range $(-\frac{1}{2}\pi, \frac{1}{2}\pi]$.

If the container is infinitely long the condition that θ_D and ψ_D remain finite as $x \to \pm\infty$ means that at least one of the a_{in} must be real. The lowest value of R for which this occurs is $R = R_c^\infty = \frac{27}{4}\pi^4 \approx 657{\cdot}5$ with $a = a_c = \pi/\sqrt{2}$ and $n = 1$. The corresponding disturbance is then given by

$$\theta_D = A \cos a_c x + B \sin a_c x, \quad \psi_D = C \cos a_c x + D \sin a_c x. \tag{3.8}$$

Solutions exist for $R > R_c^\infty$ because then two of the a_i are real.

In a finite container Drazin shows that all six solutions in (3.6) are needed to satisfy the six boundary conditions (3.5), but that they may be divided into those for which θ_D, say, is even or odd in x. Thus, for the even mode with $n = 1$ we have

$$\theta_D = \sum_{i=1}^{3} A_i \cos a_i x, \quad \psi_D = \sum_{i=1}^{3} \frac{-(a_i^2 + \pi^2)}{a_i} A_i \sin a_i x, \tag{3.9}$$

and similarly for the odd mode. It may be shown that for $R < R_c^\infty$ there are again no solutions satisfying the prescribed boundary conditions and that for $R > R_c^\infty$ solutions exist only for discrete values of R. This quantization of R is, of course, to be expected because the domain is bounded. For each value of L we may calculate an infinite number of such discrete values of R and if we denote the lowest such value by $R_c(L)$ we can show that $R_c(L) \downarrow R_c^\infty$ as $L \to \infty$. The critical Rayleigh numbers for the even and odd modes will be denoted by $R_{cE}(L)$ and $R_{cO}(L)$ and are tabulated in table 1 of HW.

4. Imperfectly heated side walls

Suppose now that the vertical boundaries are no longer perfect insulators but such that

$$\partial T/\partial x = \begin{cases} \beta g(z) & \text{at} \quad x = L, & (4.1a)\\ \beta h(z) & \text{at} \quad x = -L. & (4.1b)\end{cases}$$

As in HW, we shall consider functions which can be expanded in the form

$$(g(z), h(z)) = \sum_{n=1}^{\infty} (g_n, h_n) \sin n\pi z,$$

but we shall no longer make the restriction that the boundary conditions are either even or odd in x. It is, however, convenient to write $g(z)$ and $h(z)$ in terms of odd and even functions. Then the boundary conditions are

$$\beta^{-1}\frac{\partial T}{\partial x} = \sum_{n=1}^{\infty}(g_{nO} \pm g_{nE})\sin n\pi z \quad \text{at} \quad x = \pm L, \tag{4.2}$$

where $g_{nO} = \frac{1}{2}(g_n + h_n)$ and $g_{nE} = \frac{1}{2}(g_n - h_n)$.

For $\beta \ll 1$ we expect that θ and ψ will be of the form

$$(\theta, \psi) = \sum_{n=1}^{\infty}\sum_{m=1}^{\infty}\beta^m(\theta_{mn}, \psi_{mn})\sin n\pi z, \tag{4.3}$$

where θ_{mn} and ψ_{mn} are functions of x only. If the upper and lower surfaces are free and isothermal we require

$$\theta = \psi = \partial^2\psi/\partial z^2 = 0 \quad \text{at} \quad z = 0, 1, \tag{4.4a}$$

and at the side walls we need

$$\psi = \partial\psi/\partial x = 0, \quad \partial\theta/\partial x = \beta\sum_{n=1}^{\infty}(g_{nO} \pm g_{nE})\sin n\pi z \quad \text{at} \quad x = \pm L. \tag{4.4b}$$

This suggests that we further write

$$(\theta_{mn}, \psi_{mn}) = (\theta_{Omn} + \theta_{Emn}, \psi_{Omn} + \psi_{Emn}), \tag{4.5}$$

where θ_{Omn} is odd in x and θ_{Emn} is even. Then if we substitute the expansions (4.3) and (4.5) into (2.1) and (2.2) and equate terms in $\beta \sin n\pi z$ to zero we obtain

$$\left.\begin{aligned} \mathscr{L}_n\theta_{O1n} - \psi'_{O1n} = \mathscr{L}_n^2\psi_{O1n} - R\theta'_{O1n} = 0, \\ \psi_{O1n} = \psi'_{O1n} = 0, \quad \theta'_{O1n} = g_{nO} \quad \text{at} \quad x = \pm L \end{aligned}\right\} \tag{4.6}$$

and

$$\left.\begin{aligned} \mathscr{L}_n\theta_{E1n} - \psi'_{E1n} = \mathscr{L}_n^2\theta_{E1n} - R\theta'_{E1n} = 0, \\ \psi_{E1n} = \psi'_{E1n} = 0, \quad \theta'_{E1n} = \pm g_{nE} \quad \text{at} \quad x = \pm L. \end{aligned}\right\} \tag{4.7}$$

Here the operator $\mathscr{L}_n$ is defined by $\mathscr{L}_n = d^2/dx^2 - n^2\pi^2$ and a prime denotes d/dx.

The solution to the even inhomogeneous problem defined in (4.7) was given in HW and was shown to be unique provided that $R < R_{cE}(L)$. As R approaches $R_{cE}(L)$ the amplitude of the solution grows like $(R - R_{cE})^{-1}$ until nonlinear forces come into play to restrict further increases in amplitude. A balance between nonlinear effects and resonance effects occurs when

$$R - R_{cE} \sim \gamma^{\frac{2}{3}},$$

where $\gamma = \beta L^{-2}$, and a new solution is needed in this parameter range. Similar remarks apply when the boundary conditions for θ are odd, i.e. $g_{1E} = 0$; then we denote the critical Rayleigh number by $R_{cO}(L)$. In both cases it is the first, $n = 1$, mode that is resonated and if g_{1O} or g_{1E} is non-zero this is the only mode we need consider. On the other hand if $g_{1O} = g_{1E} = 0$ but g_{nO} or g_{nE} is non-zero for some $n > 1$ then higher modes are excited. We shall exclude that possibility from the present discussion and set $n = 1$ hereafter.

We shall show later that for some values of L these solutions are valid as long as $R - \min\{R_{cO}, R_{cE}\} \sim \gamma^{\frac{2}{3}}$, but for others the theory given in HW needs some modification. That theory breaks down completely when the boundary conditions are neither

odd nor even, for both modes are forced and are coupled when nonlinear effects are taken into account. The object of this paper is to fill in these gaps in the theory.

In the neighbourhood of R_{cO} let us write R in the form

$$R = R_{cO}(1+\gamma^{\frac{2}{3}}R_1), \tag{4.8}$$

where $R_1 \sim 1$, and further define μ as a measure of $R_{cE}-R_{cO}$ by writing

$$R_{cE} = R_{cO}(1+\gamma^{\frac{2}{3}}\mu). \tag{4.9}$$

Then if $\mu < 0$ the even mode resonates first and if $\mu > 0$ the odd mode does so.

The parameter γ is taken to be small, but is so far otherwise unspecified. It is convenient to define it in such a way as to make $\mu \sim 1$ for the range of values of L under examination. Accordingly let us take

$$\gamma^{\frac{2}{3}} = \max_L |R_{cE}-R_{cO}|/R_{cO}.$$

It was shown in HW that although the sign of $\mu(R_{cE}-R_{cO})/R_{cO}$ changes with L its magnitude is small for moderate values of L and $O(L^{-3})$ for $L \gg 1$. The magnitude of the imperfection in the boundary conditions is therefore $O(\gamma L^2 \max(g_{1O}, g_{1E}))$ and we shall take g_{1O} and g_{1E} to be $O(L^{-2})$. It was shown in HW that this solution is valid only if $R_1\gamma^{\frac{2}{3}} \ll L^{-2}$, for large values of L. This is consistent with the scaling adopted above provided that R_1 is no larger than $O(L)$ as $L \to \infty$. We shall take R_1 to be $O(1)$.

So far we have sought neutrally stable solutions. When the boundaries are perfect insulators such a solution is possible if $R_1 < \min(R_{cO}, R_{cE})$ but thereafter nonlinear effects give rise to a growth rate $O(R_1 - \min(R_{cO}, R_{cE}))$. This suggests that we adopt a new scaling for t by writing $t = \gamma^{-\frac{2}{3}}T$ so that $\partial/\partial t = \gamma^{\frac{2}{3}}\partial/\partial T$; we then take $\partial/\partial T$ to be $O(1)$.

We also expand θ and ψ in powers of γ. Following HW, we write

$$(\theta, \psi) = \gamma^{\frac{1}{3}}(\tilde{\theta}_{\frac{1}{3}}, \tilde{\psi}_{\frac{1}{3}}) + \gamma^{\frac{2}{3}}(\tilde{\theta}_{\frac{2}{3}}, \tilde{\psi}_{\frac{2}{3}}) + \gamma(\tilde{\theta}_1, \tilde{\psi}_1) + O(\gamma^{\frac{4}{3}}). \tag{4.10}$$

When we substitute the above expansions into (2.1) and equate terms of order $\gamma^{\frac{1}{3}}$ we find that

$$(\tilde{\theta}_{\frac{1}{3}}, \tilde{\psi}_{\frac{1}{3}}) = [A(L,T)(\theta_E, \psi_E) + B(L,T)(\theta_O, \psi_O)]\sin \pi z, \tag{4.11}$$

where $A(L,T)$ and $B(L,T)$ are functions of L and T to be determined and (θ_E, ψ_E) and (θ_O, ψ_O) satisfy

$$\left.\begin{aligned} \mathscr{L}_1\theta_E - \psi'_E = \mathscr{L}_1^2\psi_E - R_E\theta'_E = 0, \\ \mathscr{L}_1\theta_O - \psi'_O = \mathscr{L}_1^2\psi_O - R_O\theta'_O = 0, \\ \psi_E = \psi'_E = \theta'_E = \psi_O = \psi'_O = \theta'_O = 0 \quad \text{at} \quad x = \pm L. \end{aligned}\right\} \tag{4.12}$$

Then (θ_E, ψ_E) and (θ_O, ψ_O) are the first even and odd modes of the corresponding homogeneous problem defined in (3.4) and (3.5). Details of the solution of (4.12) are given in appendix A.

At order $\gamma^{\frac{2}{3}}$ we find that

$$(\tilde{\theta}_{\frac{2}{3}}, \tilde{\psi}_{\frac{2}{3}}) = [A^2(\theta_{20}, \psi_{20}) + B^2(\theta_{21}, \psi_{21}) + AB(\theta_{22}, \psi_{22})]\sin 2\pi z, \tag{4.13}$$

where

$$\left.\begin{aligned} \mathscr{L}_2\theta_{20} - \psi'_{20} = \tfrac{1}{2}\pi\{\theta'_E\psi_E - \theta_E\psi'_E\}, \\ \mathscr{L}_2^2\psi_{20} - R_{cE}\theta'_{20} = (\pi/2\sigma)(\mathscr{L}_1\psi'_E\psi_E - \mathscr{L}_1\psi_E\psi'_E\}, \end{aligned}\right\} \tag{4.14}$$

$$\left.\begin{aligned} \mathscr{L}_2\theta_{21} - \psi'_{21} = \tfrac{1}{2}\pi(\psi_O\theta'_O - \theta_O\psi'_O), \\ \mathscr{L}_2^2\psi_{21} - R_{cE}\theta'_{21} = (\pi/2\sigma)(\psi_O\mathscr{L}_1\psi'_O - \psi'_O\mathscr{L}_1\psi_O), \end{aligned}\right\} \tag{4.15}$$

$$\left.\begin{aligned}\mathscr{L}_2\theta_{22}-\psi'_{22} &= \tfrac{1}{2}\pi(\psi_O\theta'_E+\psi_E\theta'_O-\theta_E\psi'_O-\theta_O\psi'_E),\\ \mathscr{L}_2^2\psi_{22}-R_{cO}\theta'_{22} &= (\pi/2\sigma)(\psi_O\mathscr{L}_1\psi'_E+\psi_E\mathscr{L}_1\psi'_O-\psi'_O\mathscr{L}_1\psi_E-\psi'_E\mathscr{L}_1\psi_O)\end{aligned}\right\} \tag{4.16}$$

and $\psi_{2i}=\psi'_{2i}=\theta'_{2i}=0$ at $x=\pm L$ $(i=0,1,2)$.

It can be seen from the terms on the right-hand sides of these equations that θ_{20}, θ_{21} and ψ_{22} are even functions of x while ψ_{20}, ψ_{21} and θ_{22} are odd functions. The choice of R_{cE} or R_{cO} in the left-hand sides has been made accordingly but since they differ by a term $O(\gamma^{\frac{3}{2}})$ the choice is arbitrary at this order. The function pair (θ_{20},ψ_{20}) is identical to the pair $(\tilde{\theta}_{\frac{2}{3}},\tilde{\psi}_{\frac{2}{3}})$ given in HW and all the functions (θ_{2i},ψ_{2i}) $(i=0,1,2)$ are given in appendix A.

At order γ we see that

$$(\tilde{\theta}_1,\tilde{\psi}_1)=(\theta_3,\psi_3)\sin\pi z+(\theta_4,\psi_4)\sin 3\pi z, \tag{4.17}$$

where, in particular,

$$\left.\begin{aligned}\mathscr{L}_1\theta_3-\psi'_3 &= A^3F_0(x)+A^2BF_1(x)+AB^2F_2(x)+B^3F_3(x)\\ &\quad+\sigma(dA/dT)\theta_E+\sigma(dB/dt)\theta_O,\\ \mathscr{L}_1^2\psi_3-R_{cO}\theta'_3 &= A^3G_0(x)+A^2BG_1(x)+AB^2G_2(x)+B^3G_3(x)\\ &\quad+R_{cO}R_1(A\theta'_E+B\theta'_O)+(dA/dT)\mathscr{L}_1\psi_E+(dB/dt)\mathscr{L}_1\psi_O,\end{aligned}\right\} \tag{4.18}$$

with $$\psi_3=\psi'_3=\theta'_3=0 \quad \text{at} \quad x=\pm L.$$

Here the functions $F_i(x)$ and $G_i(x)$ $(i=0,1,2,3)$ are defined in terms of θ_E, ψ_E, etc. and are given in appendix B.

The boundary conditions are

$$\psi_3=\psi'_3=0, \quad \theta'_3=L^2(g_{1O}\pm g_{1E}) \quad \text{at} \quad x=\pm L. \tag{4.19}$$

We note that F_0, F_2, G_0 and G_2 are even functions of x while F_1, F_3, G_1 and G_3 are odd functions and again the choice of R_{cE} or R_{cO} on the left-hand side of (4.18) is arbitrary. The boundary conditions (4.19) also consist of odd and even terms and it is convenient to split θ_3 and ψ_3 into their odd and even components by writing

$$(\theta_3,\psi_3)=(\theta_{3E},\psi_{3E})+(\theta_{3O},\psi_{3O}),$$

where

$$\left.\begin{aligned}\mathscr{L}_1\theta_{3E}-\psi'_{3E} &= A^3F_0(x)+AB^2F_2(x)+\sigma(dA/dt)\theta_E,\\ \mathscr{L}_1^2\psi_{3E}-R_{cE}\theta'_{3E} &= A^3G_0(x)+AB^2G_2(x)+R_{cO}(R_1-\mu)\,d\theta_E/dx\\ &\quad+(dA/dt)\mathscr{L}_1\psi_E,\\ \psi_{3E}=\psi'_{3E}&=0, \quad \theta'_{3E}=\pm L^2g_{1E} \quad \text{at} \quad x=\pm L\end{aligned}\right\} \tag{4.20}$$

and

$$\left.\begin{aligned}\mathscr{L}_1\theta_{30}-\psi'_{30} &= B^3F_3(x)+BA^2F_1(x)+\sigma(dB/dt)\theta_O,\\ \mathscr{L}_1^2\psi_{30}-R_{cO}\theta'_{30} &= B^3G_3(x)+BA^2G_1(x)+BR_1R_{cO}\,d\theta_O/dx+(dB/dt)\mathscr{L}_1\psi_O,\\ \psi_{30}=\psi'_{30}&=0, \quad \theta'_{30}=L^2g_{10} \quad \text{at} \quad x=\pm L.\end{aligned}\right\} \tag{4.21}$$

We have written $R=R_{cE}+R_{cO}(R_1-\mu)\gamma^{\frac{1}{2}}$ in the first of these equations and equivalently $R=R_{cO}+R_{cO}R_1\gamma^{\frac{1}{2}}$ in the second. This ensures that the left-hand sides are identical to those in the linear $[O(\gamma^{\frac{1}{2}})]$ equations (4.12).

Solutions of the inhomogeneous problems defined by (4.20) and (4.21) exist provided that certain compatibility conditions are satisfied. These reduce to

$$\left.\begin{aligned}c_5\,dA/dT &= c_1(A^3+c_2AB^2-c_3(R_1-\mu)A-c_4),\\ d_5\,dB/dt &= d_1(B^3+d_2BA^2-d_3R_1B-d_4).\end{aligned}\right\} \tag{4.22}$$

The coefficients c_i and d_i $(i=1,\ldots,5)$ are defined in terms of integrals involving F_0, G_0 etc. and are given in appendix B.

5. The amplitude equation with perfect boundary conditions

We turn now to a discussion of equations (4.22) for the amplitudes A and B of the even and odd modes, and begin by considering the boundaries at $x = \pm L$ to be perfect insulators. This means that $\partial T/\partial x = 0$ at $x = \pm L$ and consequently that $c_4 = d_4 = 0$; equations (4.22) then reduce to

$$\left.\begin{aligned} c_5\, dA/dT &= c_1 A[A^2 + c_2 B^2 - c_3(R_1 - \mu)], \\ d_5\, dB/dT &= d_1 B(B^2 + d_2 A^2 - d_3 R_1). \end{aligned}\right\} \tag{5.1}$$

These equations are the same as those discussed by Keener (1976). He showed that there is a number of different classes of steady solutions depending on the relative values of the coefficients and described four such cases. In each of these there are three solutions which do not depend upon the interaction of the even and odd modes; these are

$$\left.\begin{aligned} &\text{(i)}\ \ A = B = 0 \quad \text{(trivial mode)}, \\ &\text{(ii)}\ \ A = 0, \quad B^2 = d_3 R_1, \quad R_1 > 0 \quad \text{(pure odd mode)}, \\ &\text{(iii)}\ \ B = 0, \quad A^2 = c_3(R_1 - \mu), \quad R_1 > \mu \quad \text{(pure even mode)}. \end{aligned}\right\} \tag{5.2}$$

The amplitude of the disturbance is zero for $R_1 < R_{11} = \min\{0, \mu\}$ but bifurcates at R_{11} and $R_{12} = \max\{0, \mu\}$. Keener showed that for certain values of the coefficients in (5.1) these bifurcated solutions may themselves bifurcate because of the presence of solutions of (5.1) in which neither A nor B is zero. These solutions are given by

$$\left.\begin{aligned} A^2(1 - c_2 d_2) + R_1(c_2 d_3 - c_3) + c_3 \mu &= 0, \\ B^2(1 - c_2 d_2) + R_1(d_2 c_3 - d_3) - d_2 c_3 \mu &= 0. \end{aligned}\right\} \tag{5.3}$$

The reader is referred to Keener's paper for plots of $|A^2 + B^2|^{\frac{1}{2}}$ against R_1 for each of the four cases mentioned above.

We have computed the coefficients c_1, c_2, c_3, d_1, d_2 and d_3 for L in the range (1, 10) with $\sigma = 1$. The results indicate that for certain values of L no secondary bifurcation occurs at all, in which case only the three solutions given in (5.2) are possible. A plot of $|A^2 + B^2|^{\frac{1}{2}}$ against R_1 is given in figure 1 (*a*). For all other values of L we find that the solution is Keener's case II, in which $d_2^{-1} < c_3 d_3^{-1} < c_2$ and only the mode which bifurcates second undergoes a further bifurcation. This is illustrated in Keener's figure 1, which is similar to our figure 1 (*b*). The ranges of values of L for which the solution falls into this category are given in table 1.

It was shown in HW that R_{cE} and R_{cO} depend on L in such a way that μ is positive for some values of L and negative for others. This means that for some values of L the odd mode bifurcates first and for others the even mode does so. We find that each value of L for which $\mu = 0$ lies in one of the ranges of L referred to above where a secondary bifurcation is possible, and this now enables us to describe the way the two pure modes exchange places as L passes through one of these critical values.

Suppose that L_c is one such value and suppose that (L_{1c}, L_{2c}) defines the range of L including L_c in which a secondary bifurcation is possible. Then for $L < L_{1c}$ the solution appears as in figure 1 (*a*). (We have taken μ to be positive for this illustration.) It is a straightforward matter to determine the stability of the various branches to small disturbances; we shall not give details here but the result is shown in figure 1.

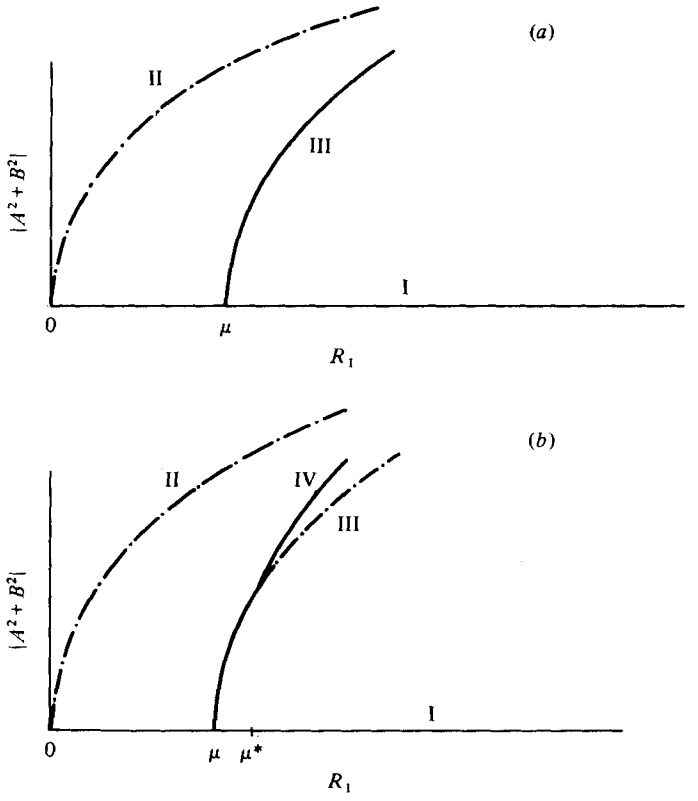

FIGURE 1. Bifurcation diagram for the perfect problem when (*a*) $L \notin (L_{1c}, L_{2c})$ and (*b*) $L \in (L_{1c}, L_{2c})$. I, $A = B = 0$; II, $A = 0$, $B = \pm (R_1 c_3 \mu)^{\frac{1}{2}}$; III, $B = 0$, $A = \pm [d_3(R_1 - \mu)]^{\frac{1}{2}}$; IV, A, B given by (5.3). μ and μ^* are defined in the text. - · - · -, stable solution; ——, unstable solution.

L_{1c}, L_{2c}	L_c	$L_{2c} - L_{1c}$	Number of cells for odd, even modes
— 1·26	1·13	—	—
1·68, 2·00	1·87	0·32	3, 2
2·43, 2·72	2·60	0·29	3, 4
3·18, 3·43	3·32	0·25	5, 4
3·92, 4·13	4·04	0·21	5, 6
4·64, 4·84	4·75	0·20	7, 6
5·36, 5·55	5·46	0·19	7, 8
6·08, 6·25	6·17	0·17	9, 8
6·80, 6·96	6·88	0·16	9, 10
7·52, 7·66	7·59	0·14	11, 10
8·23, 8·36	8·30	0·13	11, 12
8·95, 9·07	9·01	0·12	13, 12
9·66, 9·77	9·71	0·11	13, 14

TABLE 1. The ranges (L_{1c}, L_{2c}) of values of L in (1, 10) for which solutions of (5.1) bifurcate a second time. L_c is the value of L at which $R_{cE} = R_{cO}$. The Prandtl number $\sigma = 1{\cdot}0$.

When $L_{1c} < L < L_c$ the second branch bifurcates again and its secondary bifurcation is unstable, leaving the branch itself stable (figure 1*b*). Suppose that this exchange of stability occurs at $R_1 = \mu^*$. Then as $L \to L_c -$, $\mu \to 0+$ and $\mu^* \to \mu +$ with the result that the second branch approaches the first and the range of values of R_1 for which it is unstable decreases to zero. At $L = L_c$ both branches are completely stable and coalesce. As L increases further the two branches separate and change places in the diagram. Provided that $L_c < L < L_{2c}$ the branch to the right still becomes stable at some value of R_1 but for $L > L_{2c}$ it is completely unstable and the graph again resembles figure 1(*a*) but with the two pure modes interchanged. The transition of L through a critical value is then complete.

The critical values of L in (1, 10) are also given in table 1. It can be seen that at least for moderately large values of L they differ by about 0·71 and this may be interpreted in terms of the fitting of the cells into the length $2L$ of the box. For $L \gg 1$ the wavenumber is approximately that for an infinite box, $\pi/\sqrt{2}$, and this means that the wavelength is $2\sqrt{2}$. The length of each cell is therefore $\sqrt{2}$ and an extra cell is fitted in every time L is increased by $\frac{1}{2}\sqrt{2} \approx 0{\cdot}71$. The width of the range of values of L for which a secondary bifurcation occurs seems to decrease as L increases and it is expected that for large values of L the possibility of a secondary bifurcation is confined to relatively narrow ranges at intervals of about $\frac{1}{2}\sqrt{2}$. The width of this range is

$$O(|R_{cE} - R_{cO}| R_{cE}^{\frac{1}{2}} (1 - d_3/c_3 d_2)^{-1})$$

and this may be estimated for large values of L. We known that $|R_{cE} - R_{cO}|/R_{cE} \sim L^{-3}$ and $c_3, d_2, d_3 = 1 + O(L^{-2})$, so we conclude that the width of the range is $O(L^{-1})$. The number of cells associated with the odd and even modes for the range $[L_{1c}, L_{2c}]$ is shown in table 1. We note that for L in these ranges the number of cells is constant.

6. Solution of the amplitude equations

We now discuss the solutions of the amplitude equations (4.22) in the presence of the forcing terms. It is convenient to discuss separately the cases (i) $c_4 = 0$, $d_4 \neq 0$, (ii) $c_4 \neq 0$, $d_4 = 0$ and (iii) $c_4 \neq 0$, $d_4 \neq 0$. We further assume, without any loss of generality, that $\mu > 0$ so that the odd mode is the most unstable.

Case (i): $c_4 = 0$, $d_4 \neq 0$

The steady solutions of (4.22) then satisfy the equations

$$0 = A(A^2 + c_2 B^2 - c_3[R_1 - \mu]), \tag{6.1a}$$

$$0 = B^3 + d_2 B A^2 - d_3 R_1 B - d_4. \tag{6.1b}$$

Thus one solution is given by $A = 0$ and B is then determined by the cubic equation

$$0 = B^3 - d_3 R_1 B - d_4. \tag{6.2}$$

The solution of (6.2) for d_4 positive is given by curves I and II in figure 2(*a*). The first branch is stable to both odd and even disturbances whilst the second branch has an unstable part which asymptotes to zero as $R_1 \to \infty$. Curve I and the stable part of II asymptote respectively to the positive and negative roots of the equation

$$0 = B^2 - d_3 R_1 B$$

as R_1 tends to infinity.

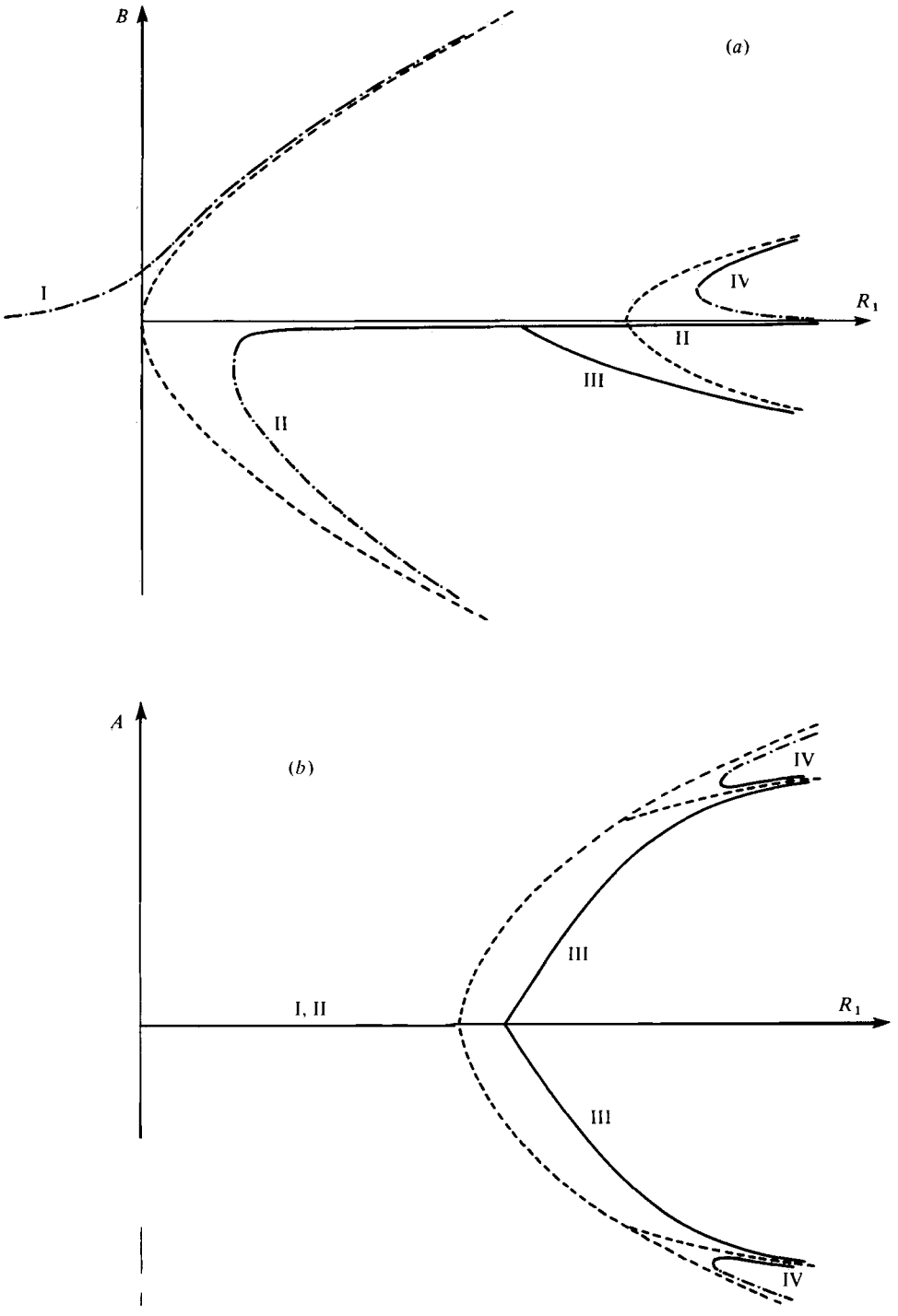

FIGURE 2. Bifurcation diagrams for steady solutions of (4.22) for case (i). (*a*) B and (*b*) A *vs.* R_1. – – – – –, perfect solutions; –·–·–, stable imperfect solutions; ——, unstable imperfect solutions. Curves I, II, III, ... are defined in the text.

Other solutions of (6.1*a*) are given by

$$0 = A^2 + c_2 B^2 - c_3[R_1 - \mu]. \tag{6.3}$$

Substitution of A^2 from (6.3) into (6.1*b*) shows that B must now satisfy the cubic equation

$$0 = B^3[1 - c_2 d_2] - B[d_3 R_1 - d_2 c_3 R_1 - d_2 c_3 \mu] - d_4. \tag{6.4}$$

We note that if $A^2 \geqslant 0$ then (6.3) gives

$$c_3[R_1 - \mu] - c_2 B^2 \geqslant 0.$$

The solutions of (6.4) satisfying the above inequality are shown as curves III and IV in figure 2(*a*). Branch III bifurcates from curve I and then asymptotes to the solution of the perfect problem as shown. The corresponding behaviour of A is shown in figure 2(*b*). We note that at the bifurcation point A is zero and dA/dR_1 is finite. Furthermore branch III is an unstable solution. The remaining solutions of (6.4) and the corresponding values of A are given by curve IV in figures 2(*a*) and (*b*). These solutions begin at a point where dA/dR_1 and dB/dR_1 are both infinite. One branch of the curves is stable and the other unstable in both cases. However, we see that if R_1 is increased from zero then the motion follows curve I unless the motion is perturbed by a disturbance sufficiently large to enable A and B to tend to the stable singular points associated with the stable parts of IV.

Case (ii): $c_4 \neq 0$, $d_4 = 0$

The steady solutions of (4.22) now satisfy the equations

$$0 = A^3 + c_2 A B^2 - c_3(R_1 - \mu) A - c_4, \tag{6.5a}$$

$$0 = B(B^2 + d_2 A^2 - d_3 R_1). \tag{6.5b}$$

We assume, without any loss of generality, that the constant c_4 is positive. We can see from (6.5) that a possible solution is $B = 0$ and that A is then determined by the equation

$$0 = A^3 - c_3(R_1 - \mu) - c_4. \tag{6.6}$$

Alternatively we can see that (6.5*b*) is satisfied if

$$B^2 = -d_2 A^2 + d_3 R_1 \tag{6.7}$$

and then A is determined by

$$0 = [1 - c_2 d_2] A^3 + A[-c_3 R_1 + c_3 \mu + c_2 d_3 R_1] - c_4. \tag{6.8}$$

If $B^2 \geqslant 0$ then solutions of (6.8) must satisfy the condition

$$d_2 A^2 < d_3 R_1.$$

The solutions of (6.6), (6.7) and (6.8) are shown in figures 3, 4 and 5. The two branches of the solution of (6.6) are shown in figures 3(*b*), 4(*b*) and 5(*b*) and are in each case labelled I and II. One solution of (6.8) is the curve III shown in each of these figures. This curve bifurcates from curve II, so that B is virtually zero on III. In addition to III, (6.8) has the solution represented by IV in figures 3(*b*), 4(*b*) and 5(*b*). We must distinguish between the following three cases:

(*a*) Curves I and IV do not intersect. This occurs when c_4 is sufficiently large and the amplitudes A and B for this case are shown in figure 3. In this case curve I is always

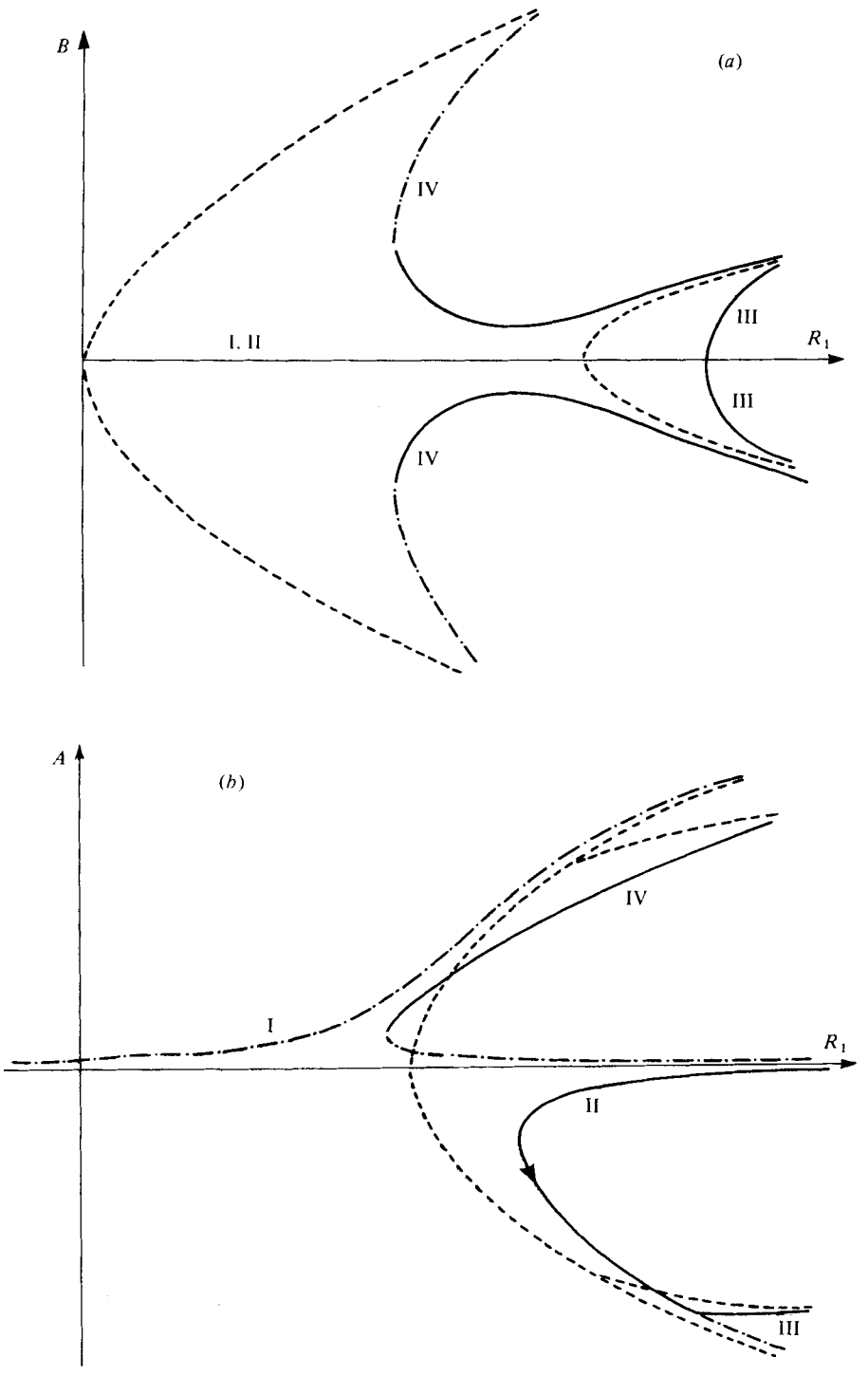

FIGURE 3. Bifurcation diagrams for steady solutions of (4.22) for case (ii*a*). Notation as in figure 2.

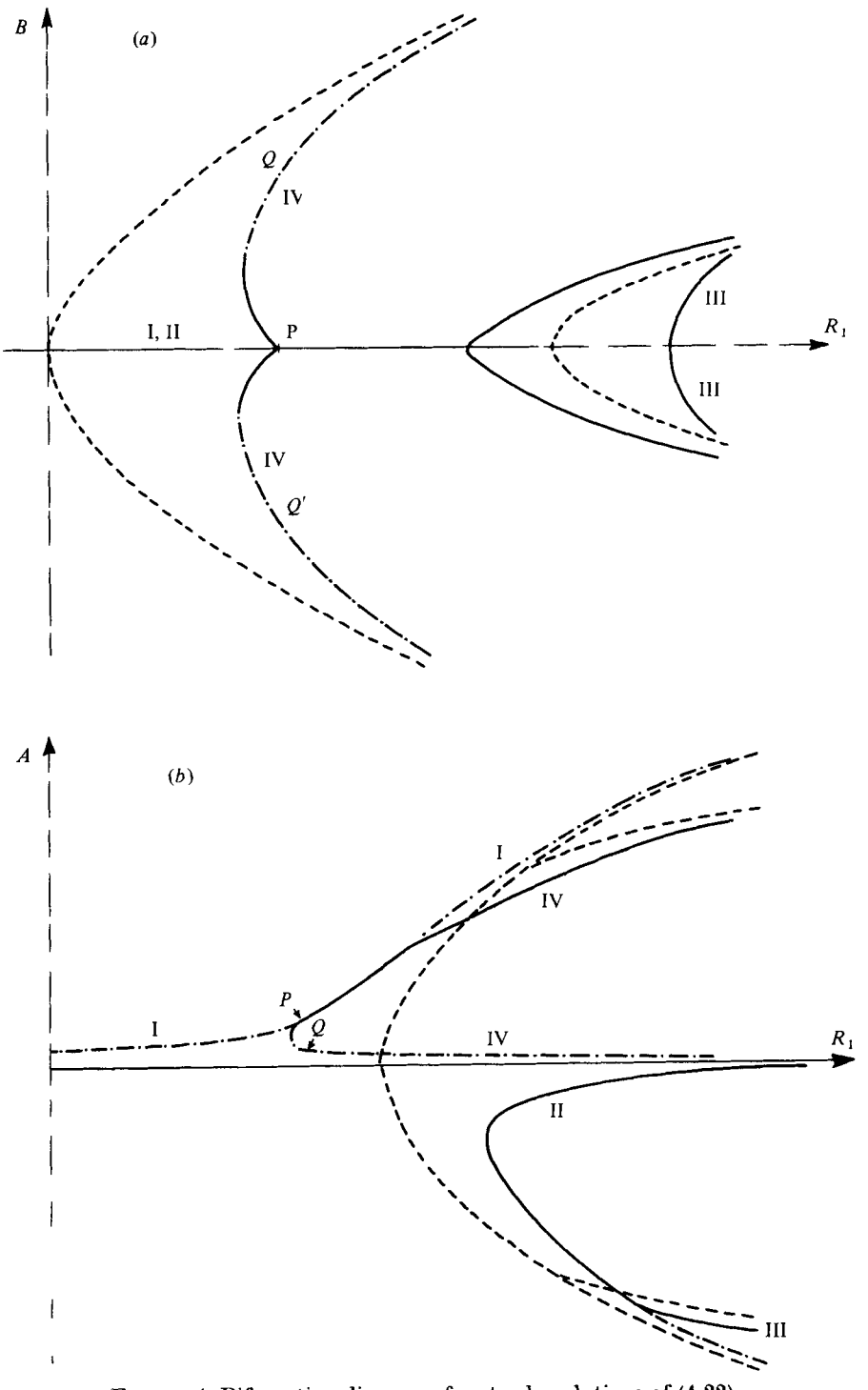

FIGURE 4. Bifurcation diagrams for steady solutions of (4.22) for case (ii*b*). Notation as in figure 2.

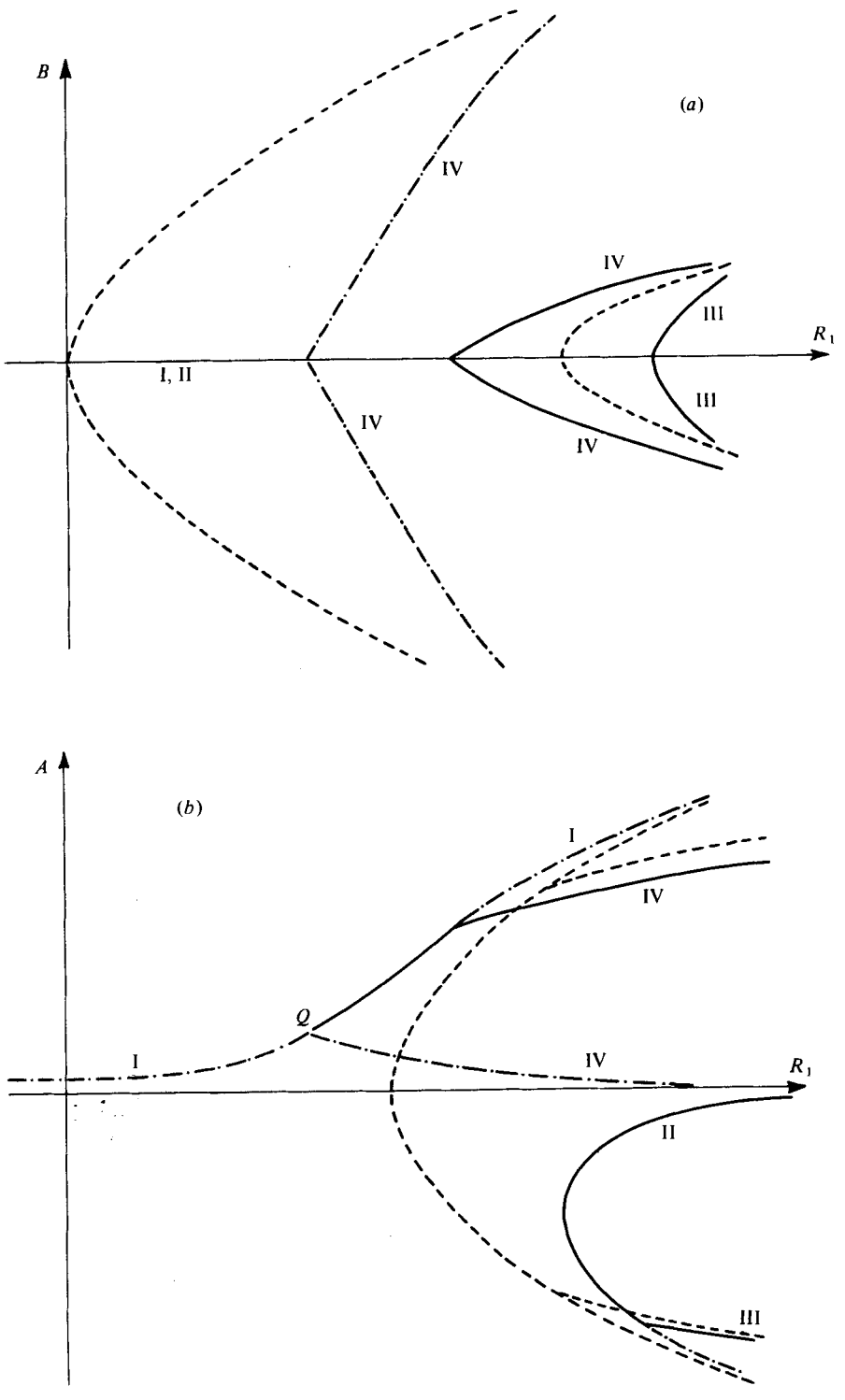

FIGURE 5. Bifurcation diagrams for steady solutions of (4.22) for case (iic). Notation as in figure 2.

stable and we see that when the Rayleigh number increases through the critical value, A asymptotes smoothly to the stable solution of the perfect problem and B remains zero.

(*b*) Curves I and IV intersect but curve IV has a point where $dA/dR_1 = 0$. This is shown in figure 4 and occurs for lower values of c_4 than does case (*a*). At the bifurcation point P where I and IV meet, I changes into an unstable solution. At this point there is no stable solution within the immediate neighbourhood of P to its right. Thus as the Rayleigh number is increased we expect that the motion will jump towards the stable steady solution at the point Q. When this occurs B jumps from P to either of the values Q or Q' shown in figure 4 (*a*). The motion after this jump has both A and B non-zero and is stable. However, as R_1 increases A tends to zero and B tends to either of the stable solutions of the perfect problem with $A = 0$.

(*c*) Curves I and IV intersect but IV has no point where $dA/dR_1 = 0$. This is shown in figure 5 and occurs for even smaller values of c_4. At the bifurcation point Q in figure 5 (*b*) the solution represented by I again becomes unstable but the motion can then follow the stable part of IV. At the bifurcation point $B = 0$ so there is no jump in this case. As the Rayleigh number increases further A tends to zero whilst B asymptotes to either of the stable solutions of the perfect problem with $A = 0$.

We conclude this subsection by noting that, if the imperfection is only in A, then provided that it is sufficiently large the motion follows the smooth path to the stable solution of the perfect problem with $B = 0$. Otherwise the motion ultimately asymptotes to the stable steady solution with $A = 0$. Furthermore, for a particular range of imperfection there is no continuous steady path to the final equilibrium state.

Case (iii): $c_4 \neq 0$, $d_4 \neq 0$

In this case the odd and even modes are both forced. The steady solutions of (4.22) then satisfy the equations

$$0 = A^3 + c_2 AB^2 - c_3(R_1 - \mu) A - c_4,$$

$$0 = B^3 + d_2 BA^2 - d_3 R_1 B - d_4.$$

We show in figure 6 typical solutions of the above equations for c_4 and d_4 both positive and of the same order of magnitude. We see that as the Rayleigh number is increased from zero the motion follows the stable path I and that as $R_1 \to \infty$ it asymptotes to the stable steady solution of the perfect problem with $A = 0$ and $B > 0$. In addition there are three other possible stable solutions at sufficiently large Rayleigh numbers each associated with portions of curves II, IV and V. Unless a finite amplitude perturbation is imposed on the flow we expect that when the Rayleigh number is increased these solutions will never be realized in practice.

We have not so far discussed the case when L lies outside the range where the perfect problem has a secondary bifurcation. In this case the solution of the perfect problem which bifurcates first is the only stable solution and the effect of the imperfections can be investigated in the manner discussed above. It suffices here to say that for all values of c_4 and d_4 the forced solution has only stable branches which asymptote to those of the perfect problem.

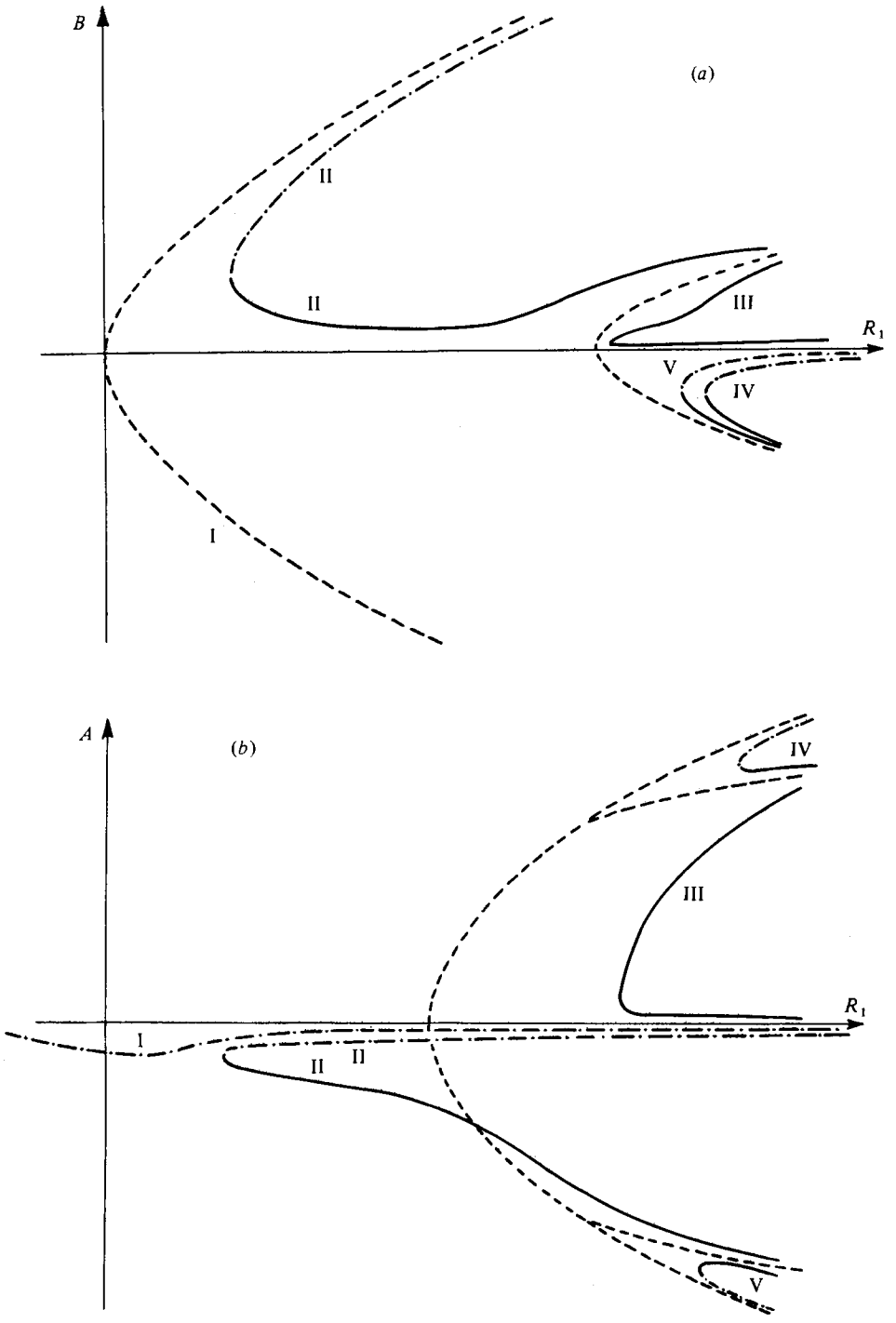

FIGURE 6. Bifurcation diagrams for steady solutions of (4.22) for case (iii). Notation as in figure 2.

Appendix A

In this appendix we give expressions for the various function pairs (θ, ψ) which satisfy (4.12) and (4.14)–(4.16). The solution of (4.12) is written in the form

$$\left.\begin{aligned} \theta_E &= \sum_{m=1}^{3} A_m \cos a_m x, \quad \psi_E = \sum_{m}^{3}{}_{1} -\frac{(a_m^2+\pi^2)}{a_m} A_m \sin a_m x, \\ \theta_O &= \sum_{m=1}^{3} C_m \sin c_m x, \quad \psi_O = \sum_{m=1}^{3} -\frac{(c_m^2+\pi^2)}{c_m} C_m \cos c_m x, \end{aligned}\right\} \tag{A 1}$$

where $$(a_m^2+\pi^2)^3 = R_{cE} a_m^2, \quad (c_m^2+\pi^2)^3 = R_{cO} c_m^2,$$

and A_m and C_m are chosen to satisfy the homogeneous boundary conditions at $x = \pm L$. The details of this calculation are given by Drazin (1975).

If we substitute the expressions (A 1) for θ_E, ψ_E, θ_O and ψ_O into (4.14) we find that

$$\begin{aligned} R_E \theta_{20} = \sum_{\substack{m=1 \\ m\neq n}}^{3} \sum_{n=1}^{3} A_m A_n [s_{mn} \cos(a_m + a_n) x + t_{mn} \cos(a_n - a_m) x] \\ + \sum_{m=1}^{3} t_{mm} A_m^2 + R_E \sum_{m=1}^{3} B_m \cos b_m x, \\ \psi_{20} = \sum_{\substack{m=1 \\ m\neq n}}^{3} \sum_{n=1}^{3} A_m A_n [\phi_{mn} \sin(a_m + a_n) x + \lambda_{mn} \sin(a_n - a_m) x] \\ - \sum_{m=1}^{3} (b_m^2 + 4\pi^2) b_m{}^1 B_m \sin b_m x, \end{aligned}$$

where

$$\begin{aligned} \phi_{mn} &= -\{(\pi/4\sigma)[(a_m+a_n)^2+4\pi^2] p_{mn} a_n^{-1} + \tfrac{1}{4}\pi R_E (a_n^2 - a_m^2)(\pi^2 - a_n a_m) a_n^{-1}\}/e_{mn}, \\ s_{mn} &= \{(\pi/4\sigma) p_{mn} a_n{}^{-1} - [(a_m+a_n)^2+4\pi^2]^2 \phi_{mn}\}/(a_m+a_n), \\ \lambda_{mn} &= -\{(\pi/4\sigma)[(a_m-a_n)^2+4\pi^2] p_{mn} a_n{}^{-1} + \tfrac{1}{4}\pi R_E (a_n^2 - a_m^2)(\pi^2 - a_n a_m) a_n^{-1}\}/d_{mn}, \\ t_{mn} &= \{(\pi/4\sigma) p_{mn} a_n{}^{-1} - [(a_m-a_n)^2+4\pi^2]^2\}/(a_n - a_m), \quad m \neq n, \\ d_{mn} &= R_E (a_n - a_m)^2 - [(a_n-a_m)^2+4\pi^2]^3, \\ e_{mn} & R_E (a_n + a_m)^2 - [(a_n+a_m)^2+4\pi^2]^3, \\ t_{mm} &= -R_E (a_m^2+\pi^2)/8\pi, \\ p_{mn} &= (a_n^2 - a_m^2)(\pi^2 + a_n^2)(\pi^2 + a_m^2). \end{aligned}$$

The constants b_m $(m = 1, 2, 3)$ are the solutions of

$$(b_m^2 + 4\pi^2)^3 = R_E b^2$$

with argument in $(-\frac{1}{2}\pi, \frac{1}{2}\pi]$. We then choose B_m $(m = 1, 2, 3)$ such that the homogeneous boundary conditions are satisfied at $x = L$.

Similarly we find that the solution of (4.15) is

$$\begin{aligned} R_E \theta_{21} = \sum_{\substack{m=1 \\ m\neq n}}^{3} \sum_{n=1}^{3} C_m C_n [u_{mn} \cos(c_m + c_n) x + v_{mn} \cos(a_m - a_n) x] \\ + \sum_{m=1}^{3} v_{mn} C_m^2 + R_E \sum_{m=1}^{3} D_m \cos b_m, \end{aligned}$$

$$\psi_{21} = \sum_{m=1}^{3}\sum_{n=1}^{2} C_m C_n[\mu_{mn}\sin[c_m+c_n)\,x - \nu_{mn}\sin(a_m-a_n)\,x] - \sum_{m=1}^{3}(b_m^2+\pi)\,b_m^{-1}\,D_m\sin b_m.$$

Here $u_{mn} = -s_{mn}$, $\mu_{mn} = -\phi_{mn}$, $\nu_{mn} = t_{mn}$ and $v_{mn} = \lambda_{mn}$ but with a_m and a_n replaced by c_m and c_n respectively. The constants D_m $(m = 1, 2, 3)$ are chosen to satisfy the homogeneous boundary conditions at $x = L$.

From (4.16) we find that

$$R_O\theta_{22} = \sum_{m=1}^{3}\sum_{n=1}^{3} A_m C_n[w_{mn}\sin(a_m+c_n)\,x + z_{mn}\sin(a_m-c_n)\,x] + \sum_{m=1}^{3} R_O E_m \sin d_m x,$$

$$\psi_{22} = \sum_{m=1}^{3}\sum_{n=1}^{3} A_m C_n[\omega_{mn}\cos(a_m+c_n)\,x + \zeta_{mn}\cos(a_m \quad c_n)\,x] + \sum_{m=1}^{3}(d_m^2+4\pi^2)\,d_m^{-1}\,E_m\cos d_m x,$$

where

$$\omega_{mn} = \{\tfrac{1}{4}\pi R_O(c_n a_m - \pi^2)(a_m^2-c_n^2)\,c_{\ n}{}^{1}a_m^{-1} - (\pi/4\sigma)\,q_{mn}[(a_m+c_n)^2+4\pi^2]\}\,(a_m-c_n)/f_{mn},$$

$$w_{mn} = \{\omega_{mn}[(a_m+c_n)^2+4\pi^2]^2 - (a_m-c_n)\,(\pi/4\sigma)\,q_{mn}\}/(a_m+c_n),$$

$$\zeta_{mn} = \{(\pi/4\sigma)\,[(a_m-c_n)^2+4\pi^2]q_{mn} - \tfrac{1}{4}R_O\pi(a_m c_n+\pi^2)\,(a_m^2-c_n^2)\,a_m^{-1}c_n^{-1}\}\,(a_m+c_n)/g_{mn},$$

$$z_{mn} = \{[(a_m-c_n)^2+4\pi^2)^2\,\zeta_{mn} - (\pi/4\sigma)\,(a_m+c_n)\,q_{mn}\}/(a_m-c_n),$$

$$f_{mn} = R_O(a_m+c_n)^2 - [(a_m+c_n)^2+4\pi^2]^3,$$

$$g_{mn} = R_O(a_m-c_n)^2 - [(a_m-c_n)^2+4\pi^2]^3,$$

$$q_{mn} = (a_m^2-c_n^2)\,(a_m^2+\pi^2)\,(c_n^2+\pi^2)/a_m c_n.$$

The constants d_m $(m = 1, 2, 3)$ are the solutions of

$$(d^2+4\pi^2)^3 = R_O d^2$$

with argument in $(-\frac{1}{2}\pi, \frac{1}{2}\pi]$ and the E_m $(m = 1, 2, 3)$ are chosen to satisfy the homogeneous boundary conditions at $x = L$.

Appendix B

The functions $F_i(x)$ and $G_i(x)$ $(i = 0, 1, 2, 3)$ used in (4.18) are defined by

$$F_0(x) = \tfrac{1}{2}\pi[\psi_E\theta'_{20} - 2\psi_{20}\theta'_E + 2\theta_{20}\psi'_E - \theta_E\psi'_{20}],$$

$$F_1(x) = \tfrac{1}{2}\pi[\psi_O\theta'_{20} + \psi_E\theta'_{22} - 2\psi_{20}\theta'_O - 2\psi_{22}\theta'_E + 2\theta_{20}\psi'_O + 2\theta_{22}\psi'_E - \theta_E\psi'_{22} - \theta_O\psi'_{20}],$$

$$F_2(x) = \tfrac{1}{2}\pi[\psi_E\theta'_{21} + \psi_O\theta'_{22} - 2\psi_{21}\theta'_E - 2\psi_{22}\theta'_O + 2\theta_{21}\psi'_E + 2\theta_{22}\psi'_O - \theta_O\psi'_{22} - \theta_E\psi'_{21}],$$

$$F_3(x) = \tfrac{1}{2}\pi[\psi_O\theta'_{21} - 2\psi_{21}\theta'_O + 2\theta_{21}\psi'_O - \theta_O\psi'_{21}],$$

$$G_0(x) = (\pi/2\sigma)\,[\psi_E\mathscr{L}_2\psi'_{20} - 2\psi_{20}\mathscr{L}_1\psi'_E + 2\psi'_E\mathscr{L}_2\psi_{20} - \psi'_{20}\mathscr{L}_1\psi_E],$$

$$G_1(x) = (\pi/2\sigma)[\psi_O \mathscr{L}_2 \psi'_{20} + \psi_E \mathscr{L}_2 \psi'_{22} - 2\psi_{20} \mathscr{L}_1 \psi'_O - 2\psi_{22} \mathscr{L}_1 \psi'_E + 2\psi'_O \mathscr{L}_2 \psi_{20} + 2\psi'_E \mathscr{L}_2 \psi_{22} - \psi'_{20} \mathscr{L}_1 \psi_O - \psi'_{22} \mathscr{L}_1 \psi_E],$$

$$G_2(x) = (\pi/2\sigma)[\psi_O \mathscr{L}_2 \psi'_{22} + \psi_E \mathscr{L}_2 \psi'_{21} = 2\psi_{21} \mathscr{L}_1 \psi'_E - 2\psi_{22} \mathscr{L}_1 \psi'_O + 2\psi'_E \mathscr{L}_2 \psi_{21} + 2\psi'_O \mathscr{L}_2 \psi_{22} - \psi'_{22} \mathscr{L}_1 \psi_O - \psi'_{21} \mathscr{L}_1 \psi_E],$$

$$G_3(x) = (\pi/2\sigma)[\psi_O \mathscr{L}_2 \psi'_{21} - 2\psi_{21} \mathscr{L}_1 \psi'_O + 2\psi'_O \mathscr{L}_2 \psi_{21} - \psi'_{21} \mathscr{L}_1 \psi_O].$$

The coefficients c_i and d_i ($i = 1, \ldots, 5$) used in (5.3) are defined by

$$c_1 = 2\int_0^L [F_0(x) R_{cE} \theta_E - G_0(x) \psi_E]\, dx,$$

$$c_2 = 2c_1^{-1} \int_0^L [F_2(x) R_{cE} \theta_E - G_2(x) \psi_E]\, dx,$$

$$c_3 = 2c_1^{-1} R_{cO} \int_0^L (d\theta_E/dx) \psi_E\, dx,$$

$$c_4 = 2c_1^{-1} L^2 g_{1E} R_{cE} \theta_E(L), \quad c_5 = -2\int_0^L (\sigma R_{cE} \theta_E^2 - \psi_E \mathscr{L}_1 \psi_E)\, dx,$$

$$d_1 = 2\int_0^L [F_3(x) R_{cO} \theta_O - G_3(x) \psi_O]\, dx,$$

$$d_2 = 2d_1^{-1} \int_0^L [F_1(x) R_{cO} \theta_O - G_1(x) \psi_O]\, dx,$$

$$d_3 = 2d_1^{-1} R_{cO} \int_0^L \frac{d\theta_O}{dx} \psi_O\, dx, \quad d_4 = 2d_1^{-1} L^2 g_{1O} R_{cO} \theta_O(L),$$

$$d_5 = -2\int_0^L (\sigma R_{cO} \theta_O^2 - \psi_O \mathscr{L}_1 \psi_O)\, dx.$$

REFERENCES

DANIELS, P. G. 1977 The effect of distant sidewalls on finite amplitude Bénard convection. *Proc. Roy. Soc.* A **358**, 173–197.

DRAZIN, P. G. 1975 On the effects of side walls on Bénard convection. *Z. angew. Math. Phys.* **27**, 239–243.

HALL, P. & WALTON, I. C. 1977 The smooth transition to a convective regime in a two-dimensional box. *Proc. Roy. Soc.* A **358**, 199–221.

KEENER, J. P. 1976 Secondary bifurcations in non-linear diffusion reaction equations. *Stud. Appl. Math.* **55**, 187–211.

KELLY, R. E. & PAL, D. 1976 Thermal convection induced between non-uniformly heated horizontal surfaces. *Proc.* 1976 *Heat Transfer Fluid Mech. Inst.* pp. 1–17. Stanford University Press.